

# Dephasing and interwell transitions in double quantum well heterostructures

G. M. Minkov,<sup>1,2</sup> A. V. Germanenko,<sup>2</sup> O. E. Rut,<sup>2</sup> A. A. Sherstobitov,<sup>1,2</sup> A. K. Bakarov,<sup>3</sup> and D. V. Dmitriev<sup>3</sup>

<sup>1</sup>*Institute of Metal Physics, RAS, 620990 Ekaterinburg, Russia*

<sup>2</sup>*Ural State University, 620083 Ekaterinburg, Russia*

<sup>3</sup>*Institute of Semiconductor Physics, RAS, 630090 Novosibirsk, Russia*

(Received 3 August 2010; published 20 October 2010)

The interference quantum correction to the conductivity in the gated double quantum well  $\text{Al}_x\text{Ga}_{1-x}\text{As}/\text{GaAs}/\text{Al}_x\text{Ga}_{1-x}\text{As}$  structures is studied experimentally. The consistent analysis of the interference induced positive magnetoconductivity allows us to find the interwell transition time  $\tau_{12}$  and the electron dephasing time  $\tau_\phi$ . It has been obtained that  $\tau_{12}^{-1}$  resonantly depends on the difference between the electron densities in the wells as predicted theoretically. The dephasing time has been determined under the conditions when one and both quantum wells are occupied. The surprising result is that the  $\tau_\phi$  value in the one well does not depend on the occupation of the other one.

DOI: [10.1103/PhysRevB.82.165325](https://doi.org/10.1103/PhysRevB.82.165325)

PACS number(s): 73.20.Fz, 73.61.Ey

## I. INTRODUCTION

The quantum corrections to the conductivity of the two-dimensional (2D) electron gas with the single-valley parabolic energy spectrum is extensively investigated last three decades (see Refs. 1–9, and references therein). A reasonably good agreement between experimental and theoretical results evident at relatively high conductivity,  $\sigma \geq (10-15)G_0$ , where  $G_0 = e^2/\pi h$ , attests adequate understanding of the role of the quantum interference and electron-electron ( $e-e$ ) interaction in the transport properties of 2D systems. The quantum corrections in the double quantum well structures are studied significantly less.<sup>10-13</sup> Specific features of the corrections in this case are governed by relationship between the following parameters: the transport time  $\tau$ , the phase relaxation time  $\tau_\phi$ , and the interwell transition time  $\tau_{12}$ , the temperature length  $L_T = \sqrt{D/T}$  (where  $D$  is the diffusion coefficient), the interwell distance  $d$ , and the screening length  $r_0$ , which is half the Bohr radius,  $r_0 = a_B/2$ . In the limiting cases such structures can look like a single quantum well structure (at  $\tau_{12} \ll \tau_\phi, 1/T$ ) or a structure with two uncoupled wells (at  $\tau_{12} \gg \tau_\phi, 1/T$  and  $d \gg r_0$ ). In the last case, the quantum corrections to the conductivity are simply the sum of the corrections of each well, however, the crossover to this case for the weak localization and interaction corrections may occur at different conditions.

The intermediate cases are more interesting and diversified. Concerning the interaction correction, the gain of the interaction in a multiplet channel can be so significant that it can lead to the change in the sign of the temperature dependence of the conductivity from dielectric ( $d\sigma/dT > 0$ ) to metalliclike ( $d\sigma/dT < 0$ ) as it takes place in the 2D systems with double-valley energy spectrum.<sup>14</sup> The interference correction, even without interwell transitions ( $\tau_{12} \gg \tau_\phi$ ), can differ from the case of noninteracting wells due to inelasticity of the  $e-e$  interaction of carriers in the different wells. This interaction can change the dephasing rate significantly. Just this effect in the gated double quantum well  $\text{Al}_x\text{Ga}_{1-x}\text{As}/\text{GaAs}/\text{Al}_x\text{Ga}_{1-x}\text{As}$  structures is studied in the present paper. Analyzing the interference-induced positive magnetoconductivity we show that the interwell transition

rate resonantly depends on the gate voltage. We also show that the dephasing rate is almost insensitive to the number of the wells occupied contrary to the theoretical expectations.

## II. EXPERIMENTAL DETAILS

Two structures grown by the molecular-beam epitaxy on a semi-insulating GaAs substrate were investigated. The first structure 3243 consists of 200-nm-thick undoped GaAs buffer layer, 50 nm undoped  $\text{Al}_{0.3}\text{Ga}_{0.7}\text{As}$  layer, two 8 nm GaAs quantum wells separated by 10 nm  $\text{Al}_{0.3}\text{Ga}_{0.7}\text{As}$  barrier, and 70 nm  $\text{Al}_{0.3}\text{Ga}_{0.7}\text{As}$  undoped layer. The thickness of the GaAs cap layer is 130 nm. The main doping  $\delta$  layer of Si is situated in the barrier center. Because the gate voltage in such a type of structures can effectively decrease the electron density only, an additional Si  $\delta$  layer is located above the upper quantum well at distance of 18 nm from the well interface. The energy diagram of the structure 3243 is shown in Fig. 1. The second structure 3154 differs by the doping level and has lower electron density and mobility. Such structure design allows us to have the close mobilities in the wells at equal electron density that is very important for reliable determination of the phase relaxation time as will be discussed below. The samples were mesa etched into standard Hall bars

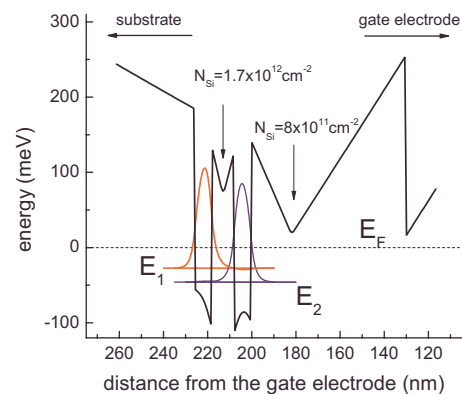


FIG. 1. (Color online) The energy diagram of the structure 3243 for  $V_g = 0$ .

and then an Al gate electrode was deposited by thermal evaporation onto the cap layer through a mask. All the measurements were carried out in the Ohmic regime using dc technique. The results for both structures were mostly analogous and we will discuss more thoroughly the results obtained for the structure 3243.

### III. RESULTS AND DISCUSSION

The shape of magnetoconductivity  $\Delta\sigma(B)$  caused by suppression of the weak localization in the transverse magnetic field  $B\parallel n$ , where  $n$  is the normal to the structure plane, is widely varied in the double well structures. Really, even in the case of low interwell transition rate, when  $\Delta\sigma(B)$  is barely the sum of the contributions from each well

$$\begin{aligned} \frac{\Delta\sigma(B)}{G_0} &= \frac{\rho_{xx}^{-1}(B) - \rho_{xx}^{-1}(0)}{G_0} \\ &= \alpha_1 \mathcal{H}\left(\frac{\tau_{\phi 1}}{\tau_1} \frac{B}{B_{tr 1}}\right) + \alpha_2 \mathcal{H}\left(\frac{\tau_{\phi 2}}{\tau_2} \frac{B}{B_{tr 2}}\right), \end{aligned} \quad (1)$$

it depends, as seen, on the large number of parameters: the two phase relaxation times,  $\tau_{\phi 1}$  and  $\tau_{\phi 2}$ , the two transport times,  $\tau_1$  and  $\tau_2$ , and two transport magnetic fields,  $B_{tr 1} = \hbar/4eD_1\tau_1$  and  $B_{tr 2} = \hbar/4eD_2\tau_2$ . The remaining designations in Eq. (1) are the following:

$$\mathcal{H}(x) = \psi\left(\frac{1}{2} + \frac{1}{x}\right) + \ln x, \quad (2)$$

where  $\psi(x)$  is a digamma function,  $\alpha_1$  and  $\alpha_2$  are prefactors, which appear due to not rigorous fulfillment of the diffusion approximation  $\tau_i/\tau_{\phi i} \ll 1$ ,<sup>15</sup>  $i=1,2$ , due to the magnetic field dependence of the dephasing time<sup>16</sup> and the contributions of the second-order corrections.<sup>17</sup> Obviously it is impossible to find six parameters while fitting the single smooth curve. Reliable obtaining of the phase relaxation time is possible only when the corresponding parameters  $\tau_i$ ,  $\tau_{\phi i}$ , and  $B_{tr i}$  in the wells are close to each other. Therefore, before to inspect interference-induced low-field magnetoconductivity let us analyze the transport in high magnetic field in more detail.

The magnetic field dependences of the Hall coefficient  $R_H = \rho_{xy}/B$  and transverse resistivity  $\rho_{xx}$  for the different gate voltages are presented in Fig. 2. First we analyze the Shubnikov-de Haas (SdH) oscillations. As seen the oscillations picture is rather complicated at some gate voltages that stems from the difference in the electron densities,  $n_1$  and  $n_2$ , in the wells. The  $V_g$  dependences of the  $n_1$  and  $n_2$  values obtained from the Fourier analysis are shown in Fig. 3(a) by circles. One can see that  $n_1$  and  $n_2$  linearly decrease with the  $V_g$  decrease. Therewith, the decrease rate for one of the wells at  $V_g \geq -4$  V is about 15 times larger than that for other one:  $dn_2/dV_g \approx 2.8 \times 10^{11} \text{ cm}^{-2}/\text{V}$  against  $dn_1/dV_g \approx 2 \times 10^{10} \text{ cm}^{-2}/\text{V}$ . Both values are in agreement with the results of simple estimations. The rate  $dn_2/dV_g$  agrees well with the geometric capacity between the upper well and the gate electrode. The nonzero value of the rate for the lower well,  $dn_1/dV_g$ , results from the finite compressibility of the electron gas in the upper well. According to our estimates the

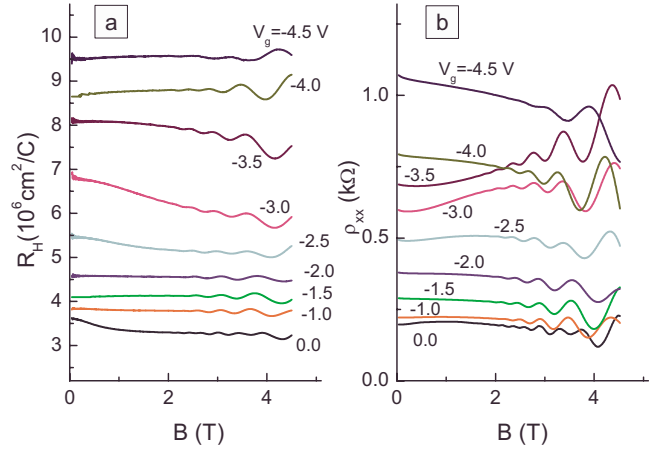


FIG. 2. (Color online) The magnetic field dependences of (a)  $R_H$  and (b)  $\rho_{xx}$  for different gate voltages,  $T=4.2$  K.

decrease rate due to this effect is about  $2.3 \times 10^{10} \text{ cm}^{-2}/\text{V}$  that is close to the experimental  $dn_1/dV_g$  value.

At  $V_g \lesssim -4$  V, the upper well is fully depleted and no longer screens the gate electric field. Therefore  $dn_2/dV_g$  is enhanced up to approximately  $2.5 \times 10^{11} \text{ cm}^{-2}/\text{V}$ , which agrees with the geometric capacity again. Thus, the analysis of the SdH oscillations shows that the structure comes to the balance, i.e., to the state when the electron densities in the wells become close to each other, at  $V_g^b = -(1.5 \pm 0.1)$  V.

As described above, to obtain  $\tau_\phi$  reliably, it is very important, besides the equal electron densities in the wells, to have the close values of the transport magnetic fields, i.e., the close values of the mobility. We used different ways to determine the mobilities. First we analyzed the monotonic run of the  $\rho_{xx}$  vs  $B$  and  $R_H$  vs  $B$  curves within the framework of the model of the classical transport accounting for two types of carriers. An example of such the data processing is shown in Figs. 3(b) and 3(c). The values of the electron densities in the wells obtained by this method [presented in Fig. 3(a) by triangles] agree well with that found from the SdH oscillations. Unfortunately, this method gives good results in the case when the mobilities differ noticeably. For the structure 3243 it happens at  $V_g \approx -(0-0.5)$  V and  $V_g \approx -(3-3.5)$  V [see Fig. 3(d)]. By assuming that  $\mu_1$  and  $\mu_2$  depend on the gate voltage monotonically, one obtains that the mobilities differ not so strongly in the balance:  $\mu_1 \approx \mu_2 = (1.5 \pm 0.1) \times 10^4 \text{ cm}^2/\text{Vs}$  at  $V_g^b = -1.5$  V.

Another way to insure that the mobilities in the wells are close in the magnitude at the balance is the detailed analysis of the SdH oscillations [see Fig. 4(a)]. If one neglects the tunneling splitting,  $\Delta_{SAS}$ , as compared with the broadening due to scattering,  $\hbar/\tau_q$ , the conductivity tensor for the structure can be represented as the sum of that for each well,

$$\sigma_j(B, V_g) = \sigma_j^{(1)}(B, V_g) + \sigma_j^{(2)}(B, V_g), \quad j = xx, xy. \quad (3)$$

The estimation of  $\Delta_{SAS}$  for our case gives the value about 0.1 meV, that is much less than  $\hbar/\tau_q \approx 5$  meV found from the  $B$  dependence of the SdH oscillations amplitude. So, such the approach seems reasonable. For the case of  $\mu_1 = \mu_2$  in the balance:  $\sigma_j^{(1)}(B, V_g^b) = \sigma_j^{(2)}(B, V_g^b) = \sigma_j(B, V_g^b)/2$ . Since the

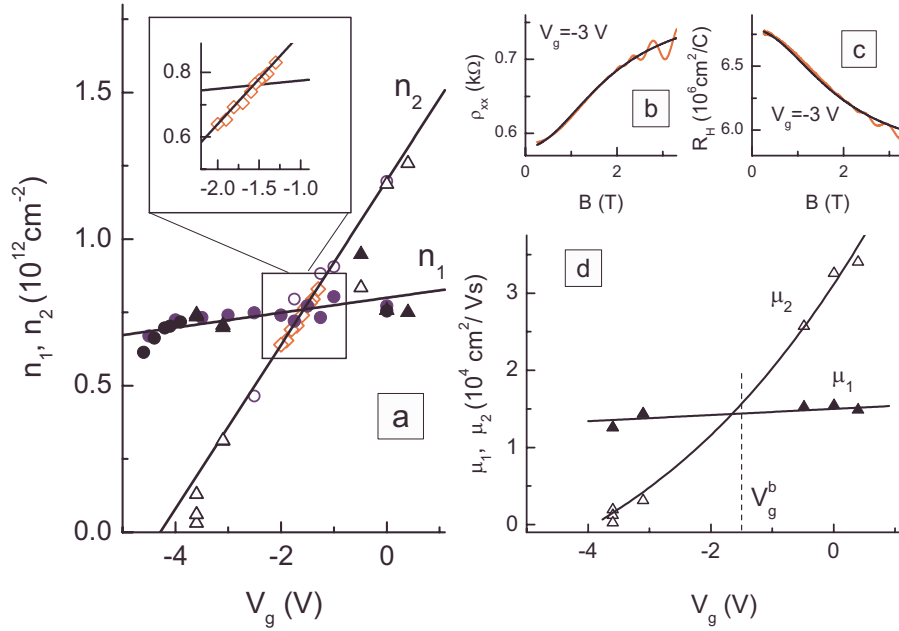


FIG. 3. (Color online) (a) The electron densities in the wells plotted against the gate voltages. The circles and diamonds are obtained from the SdH oscillations analysis, the triangles are obtained from the analysis of the monotonic run of the  $\rho_{xx}$  vs  $B$  and  $R_H$  vs  $B$  curves. [(b) and (c)] Examples of the fit of the experimental curves by the classical formula for two types carriers transport for  $V_g = -3.0 \text{ V}$ . (d) The gate voltage dependence of the mobilities in the wells obtained from the classical treatment of  $\rho_{xx}$  vs  $B$  and  $R_H$  vs  $B$  data.

electron density and mobility in the lower well are practically independent of  $V_g$  near the balance [see Fig. 3(d)], the components  $\sigma_j^{(2)}$  for the upper well can be extracted as

$$\sigma_j^{(2)}(B, V_g) = \sigma_j(B, V_g) - \frac{1}{2} \sigma_j(B, V_g^b). \quad (4)$$

The components in the right-hand side of Eq. (4) were found from the measured resistivity components  $\rho_{xx}$  and  $\rho_{xy}$ . After obtaining  $\sigma_{xx}^{(2)}$  and  $\sigma_{xy}^{(2)}$  we have calculated  $\rho_{xx}^{(2)}$  and plotted it in Fig. 4(b). Therewith, to remove the monotonic component, the  $\rho_{xx}$  vs  $B$  curves were differentiated. One can see that: (i)

the oscillations extracted are single periodic; (ii) the  $n_2$  vs  $V_g$  dependence found from the Fourier analysis is linear [see insert in Fig. 3(a)]; (iii) its slope is close to that found within whole  $V_g$  range; (iv) the oscillations amplitude is practically independent of  $V_g$  while  $V_g = -(1.7-1.3) \text{ V}$ . Such the behavior can be observed only when the mobilities in the wells at the balance,  $V_g = -1.5 \text{ V}$ , are close to each other.

Now we are ready to discuss quantitatively the low-field negative magnetoresistance caused by suppression of the weak localization. The magnetic field dependences of  $\Delta\sigma(B)$  at temperature 1.35 K for different gate voltages are presented in Fig. 5(a). At first sight all the curves are the same in the shape and no peculiarity is observed in the balance. This, indeed, should be happening when the interwell transition rate is low,  $1/\tau_{12} \ll 1/\tau_{\phi}$ , and  $\Delta\sigma(B)$  is the sum of the contributions from each well.

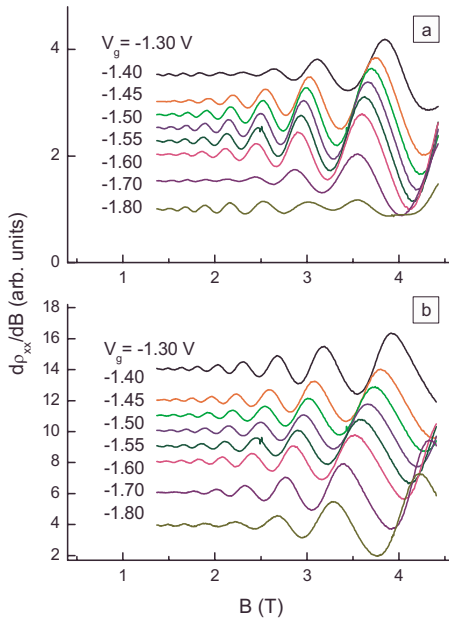


FIG. 4. (Color online) (a) The SdH oscillations of  $d\rho_{xx}/dB$  measured experimentally and (b) extracted for the upper quantum well as described in the text.

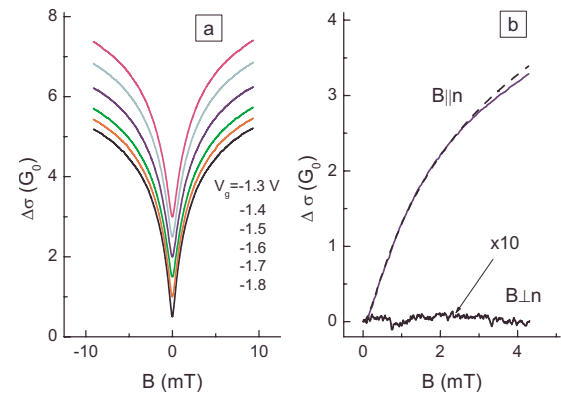


FIG. 5. (Color online) (a) The interference-induced positive magnetoconductivity for different gate voltages near the balance. For clarity, the curves are shifted in the vertical direction. (b) The magnetoconductivity measured at  $V_g = -1.5 \text{ V}$  for two orientations of the magnetic field. Solid lines are the data, the dashed line is the best fit by Eq. (5) with the parameters  $\alpha = 1.9$ ,  $\tau_{\phi}/\tau = 85$ .  $T = 1.35 \text{ K}$  for all the cases,  $B_{lr} = 8.4 \text{ mT}$ .

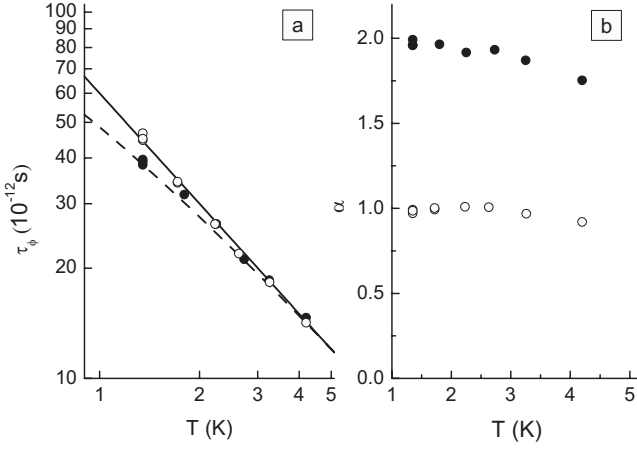


FIG. 6. The temperature dependences of (a)  $\tau_\phi$  and (b)  $\alpha$  found from the fit of the magnetoconductivity curves by Eq. (5). Solid symbols are obtained at  $V_g = -1.5$  V when the structure is in the balance. Open symbols correspond to  $V_g = -3.7$  V when the conductivity over the upper well is negligible. The solid and dashed lines are the functions  $6 \times 10^{-11}/T$  and  $(T/6.4 \times 10^{-11} + 1/2 \times 10^{-10})^{-1}$ , respectively.

Closeness of the mobilities in the balance means closeness of transport fields,  $B_{tr1} = B_{tr2} = B_{tr}$  so that  $\Delta\sigma(B)$  should be described by Eq. (1), which in this case reduces to the following:

$$\Delta\sigma(B) = \alpha G_0 \mathcal{H}\left(\frac{\tau_\phi B}{\tau B_{tr}}\right), \quad (5)$$

where  $\alpha = 2$ . Therefore, let us start analysis from  $V_g = -1.5$  V. The result of the best fit within the magnetic field range  $(0-0.3)B_{tr}$  for  $T = 1.35$  K is shown in Fig. 5(b). It is evident that Eq. (5) perfectly fits the data with the prefactor which value is really about 2. The temperature dependences of the fitting parameters  $\tau_\phi$  and  $\alpha$  are presented in Fig. 6. It is seen that the  $T$  dependence of  $\tau_\phi$  is close to  $1/T$  (some deviation will be discussed below). Slight decrease in the prefactor with the growing temperature is a consequence of the lack of the diffusion regime due to the decrease in the  $\tau_\phi$  to  $\tau$  ratio<sup>15</sup> from 85 at  $T = 1.35$  K to 30 at  $T = 4.2$  K.

Let us now analyze the data in the vicinity of  $V_g = -1.5$  V. Strictly speaking, the use of Eq. (5) is not fully correct to obtain the dephasing rate experimentally. This is because  $B_{tri}$  and  $\tau_{\phi i}/\tau_i$  are different in the wells. Nevertheless, before to discuss the workability of Eq. (5), let us consider the results of such a treatment. The gate voltage dependence of the fitting parameter  $\tau_\phi^*$  presented in Fig. 7(a) by the diamonds exhibits the sharp minimum at  $V_g = -1.5$  V (the superscript \* implies that the  $\tau_\phi$  value found from the fit can differ from the true dephasing time). To understand whether or not this minimum results from the inappropriate use of Eq. (5), we have simulated experimental situation. We have calculated the magnetoresistance using Eq. (1) with the values of  $n_i$  and  $\mu_i$  given in Fig. 3. The phase relaxation times have been calculated according to Ref. 18. Then, these curves have been fitted by Eq. (5) in the same manner as it has been done with the data. It turns out that Eq. (5) well fits the

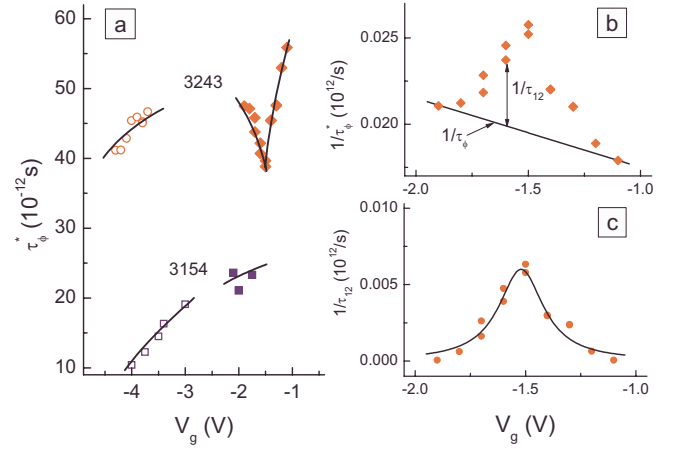


FIG. 7. (Color online) (a) The values of the fitting parameter  $\tau_\phi^*$  plotted against the gate voltage for structures 3243 and 3154. Solid symbols are obtained near the balance evident in the structures 3243 and 3154 at  $V_g^b \approx -1.5$  V and  $-2.0$  V, respectively. The open symbols correspond to the situation when only the lower quantum well contributes to the conductivity. The lines are provided as a guide to the eyes. (b) The  $1/\tau_\phi^*$  values as a function of the gate voltage for structure 3243 near the balance. (c) The gate voltage dependence of the transition rate for structure 3243. Symbols are the experimental data, the line is calculated from Eq. (7) with  $m = 0.067m_0$ ,  $dn/dV_g = 2.8 \times 10^{11}$  cm<sup>-2</sup>/V,  $\tau_{12}^b = 1.7 \times 10^{-10}$  s, and  $\tau = 5.5 \times 10^{-13}$  s.

calculated curves. Therewith, the fitting parameter  $\tau_\phi$  monotonically changes with the changing gate voltage and its value is close to  $(\tau_{\phi 1} + \tau_{\phi 2})/2$  with an accuracy of 5% in the range of the parameters corresponding to  $V_g = -(1.3 - 1.7)$  V. This means that the minimum in Fig. 7 does not bear with the fitting procedure.

It stands to reason that the minimum results from the interwell transitions neglected in Eq. (5). Theoretically, their role in the positive magnetoconductivity was considered in Refs. 10 and 11. However, our attempts to use the expressions from these papers for the data fit have failed. The values of  $\tau_\phi$  and  $\tau_{12}$  are obtained with very large uncertainty. This is because the shape of the magnetoconductivity curve in actual case is mainly controlled by some combination of  $\tau_\phi$  and  $\tau_{12}$  but not by  $\tau_\phi$  and  $\tau_{12}$  individually. It becomes clear when considering the parabolic (at  $B \rightarrow 0$ ) and logarithmic (at  $B \gg B_{tr}\tau/\tau_\phi$ ) asymptotics of Eq. (24) in Ref. 11 at  $\tau_{12} > 2\tau_\phi$ . They coincide with corresponding asymptotics, which one can extract from Eq. (5) by using  $\alpha = 2$  and  $\tau_\phi^* = (1/\tau_\phi + 1/\tau_{12})^{-1}$  instead of  $\tau_\phi$ .<sup>19</sup> So, the sum  $1/\tau_\phi + 1/\tau_{12}$ , but not the rates  $1/\tau_\phi$  and  $1/\tau_{12}$  separately are experimentally obtained when the interwell transitions are relatively rare.

According to Ref. 11, the interwell transition rate resonantly depends on the difference between the Fermi energies in the wells,

$$\frac{1}{\tau_{12}} = \frac{1}{\tau_{12}^b} \frac{1}{1 + [(E_F^1 - E_F^2)\tau/\hbar]^2}, \quad (6)$$

where  $1/\tau_{12}^b$  is the rate in the balance and  $E_F^i = \pi\hbar^2 n_i/m$  is the Fermi energy in  $i$ th well. Taking into account the fact that  $n_1$

is practically independent of  $V_g$ , one obtains the following expression:

$$\frac{1}{\tau_{12}} = \frac{1}{\tau_{12}^b} \left\{ 1 + \left[ \frac{\pi\hbar}{m} \frac{dn}{dV_g} (V_g - V_g^b) \tau \right]^2 \right\}^{-1}, \quad (7)$$

which can be directly compared with the data. Experimentally, the rate  $1/\tau_{12}$  near the balance can be found as the difference between  $1/\tau_{\phi}^*$  and  $1/\tau_{\phi}$ , if one supposes that the interwell transitions do not contribute to  $\tau_{\phi}^*$  at  $V_g = -1.8$  V and  $V_g = -1.2$  V, and  $1/\tau_{\phi}$  linearly depends on  $V_g$  between these gate voltages as shown in Fig. 7(b). The results are presented in Fig. 7(c) by the circles. As seen the experimental  $V_g$  dependence of  $1/\tau_{12}$  is really close to the theoretical one calculated from Eq. (7) with  $\tau_{12}^b = 1.7 \times 10^{-10}$  s and  $\tau = 5.5 \times 10^{-13}$  s found from the mobility value at  $V = V_g^b$  [Fig. 3(d)].

Thus, we obtain from the above analysis that the dephasing time  $\tau_{\phi}$  in the balance is about  $5 \times 10^{-11}$  s at  $T = 1.35$  K, whereas the interwell transition time is approximately three times larger,  $\tau_{12} \approx 1.7 \times 10^{-10}$  s. The fact that  $\tau_{\phi}^*$  is the combination of  $\tau_{\phi}$  inversely dependent on the temperature and  $\tau_{12}$ , which is independent of the temperature, explains the tendency to saturation of the  $\tau_{\phi}^*$  vs  $T$  dependence at low temperature [see the solid symbols and the dashed curve in Fig. 6(b)].

It is thought that the role of the interwell transitions can be independently estimated from the in-plane magnetoconductivity.<sup>11,20</sup> However, the detection of this effect is beyond accuracy of our experiment as readily illustrated by Fig. 5(b). Its magnitude can be estimated as at list 100 times less than that at  $B \parallel n$ . This agrees with the estimations made according to Ref. 11. They show that the value of the in-plane magnetoconductivity with the parameters of the structure investigated should be about 1000 times less than the value of the magnetoconductivity at  $B \parallel n$ .

It is impossible to find the values of  $\tau_{\phi 1}$  and  $\tau_{\phi 2}$  within the gate voltages range from  $-3.5$  to  $-2.0$  V because six independent parameters govern the magnetoconductivity [see discussion below Eq. (1)]. However, it can be easily done at lower gate voltage,  $V_g < -3.7$  V, when the conductivity and, thus, the magnetoconductivity are determined by the lower well only. The  $\Delta\sigma$  vs  $B$  curve for this case is well fitted by Eq. (5) with the prefactor  $\alpha$ , which value is close to 1 [see Fig. 6(b)]. Therewith the temperature dependence of  $\tau_{\phi}$ , as seen from Fig. 6(a), is close to  $1/T$ . The values of  $\tau_{\phi}$  within this gate voltage range are shown in Fig. 7(a) by the open symbols.

The same measurements were carried out on the structure 3154. The balance in this structure occurs at  $V_g = -2$  V, at the lower electron density,  $n \approx 4.5 \times 10^{11}$  cm<sup>-2</sup>, and lower mobility,  $\mu \approx 6500$  cm<sup>2</sup>/V s. The results differ by two issues. The value of  $\tau_{\phi}$  is less than that for the structure 3243. It seems natural because the conventional theory<sup>1,18</sup> predicts that  $\tau_{\phi} \propto \sigma / \ln(\sigma/G_0)$ . The second point is that the noticeable minimum at the balance is not observed [see Fig. 7(a)]. It is explained by the relatively low interwell transition rate, which is estimated<sup>11</sup> as being about two times lower than that

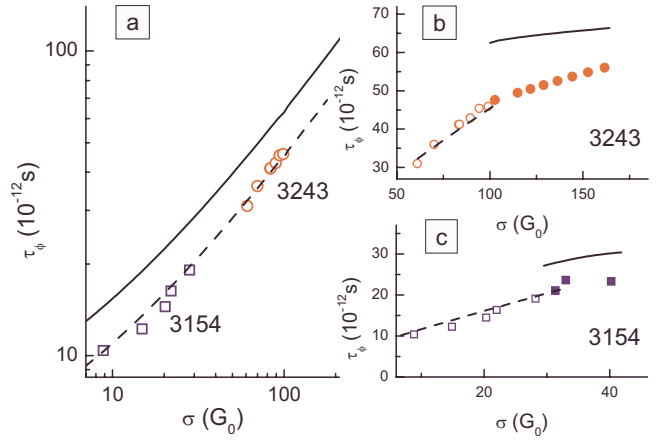


FIG. 8. (Color online) (a) The conductivity dependence of the phase relaxation time for the structure 3243 (circles) and 3154 (squares) at  $T = 1.35$  K for the case when only the lower quantum well is occupied. The solid line is calculated according to Ref. 18. The dashed line is obtained by multiplying the solid curve by the factor 0.7. [(b) and (c)] The phase relaxation time plotted against the conductivity per well for the two regimes: only the lower quantum well is occupied (open symbols, dashed lines), both quantum wells are occupied near the balance (solid symbols, solid lines). The dashed lines are calculated in the same way as in the panel (a). The solid lines are calculated from Eq. (8) with the use of  $\tau_{\phi}^{(1)}$  vs  $\sigma$  dependence shown in the panel (a) by the dashed line.

in the structure 3243 and more than six times lower than  $1/\tau_{\phi}$  at lowest temperature.

As mentioned above, the dephasing time  $\tau_{\phi}$  should mainly depend on the conductivity, at least for the single well structure. In Fig. 8(a), we show the data obtained for both structures for the case when the conductivity is determined by the one well alone. In the same figure, the theoretical dependence<sup>18</sup> is depicted by the solid line. As seen, being multiplied by the factor 0.7 it perfectly describes the data within the entire conductivity range. We believe that the appearance of the additional factor can result from the fact that the expression used for the data treatment does not take into account the magnetic field dependence of  $\tau_{\phi}$ , the contributions of the second order corrections, and the finiteness of the  $\tau_{\phi}$  to  $\tau$  ratio.

Let us again direct the reader's attention to the data obtained near the balance. These data are presented in Figs. 8(b) and 8(c) by the solid symbols. Note, they are plotted against the conductivity per one well. As seen the experimental  $\tau_{\phi}$  values obtained under the conditions, when one and both quantum wells are occupied, fall on the common curve. This means that the inelastic interaction of an electron in the one well with electrons in the other one does not contribute noticeably to the dephasing rate. At first glance the last seems very strange because the distance between the wells is about screening length so that the interaction between the carriers located in the different wells should not be significantly less than that for carriers in the one well. On the other hand, the inelastic interaction of an electron with the electrons in the other well is not sole effect influencing the dephasing rate. Another effect is an additional screening of the interaction between the electrons in the one well by the

carriers located in the other one. The former effect should lead to the  $\tau_\phi$  decrease while the second one to its increase. Theoretical calculations, which take into account both these effects, give the following expression for the dephasing time in a double layer system near the balance:<sup>21</sup>

$$\frac{\tau_\phi^{(1)}}{\tau_\phi} = \left[ 1 - \frac{1}{2} \frac{s(5 + 6d/r_0) - 1}{(1 + d/r_0)[s(3 + 2d/r_0) + 1]} \right] \frac{\ln T \tau_\phi}{\ln T \tau_\phi^{(1)}},$$

$$s = \sigma_2/\sigma_1, \quad (8)$$

where  $\sigma_1$  and  $\sigma_2$  are the conductivity of the lower and upper quantum wells, respectively,  $\tau_\phi^{(1)}$  denotes the dephasing time of a single layer, and  $d$  is the distance between the layers. Using the data in Figs. 3(a) and 3(c) for  $\sigma_1$  and  $\sigma_2$ , the distance between the centers of the wells 18 nm as the  $d$  value, the screening length  $r_0$  equal to 5 nm, and  $\tau_\phi^{(1)}(\sigma)$  shown by the dashed line in Fig. 8(a), we have calculated  $\tau_\phi$  near the balance as a function of the conductivity per one layer  $(\sigma_1 + \sigma_2)/2$  [the solid lines in Figs. 8(b) and 8(c)]. One can see that approximately 25% increase in  $\tau_\phi$  at  $T = 1.35$  K should occur according to Eq. (8) when the upper quantum well is occupied. It may appear that this change is not sufficiently large to be fixed experimentally. However, as evident from Fig. 7(a) we reliably recognize the 20% resonant dip in the  $\tau_\phi^*$  vs  $V_g$  dependence resulting from the interwell transitions but observe no change in  $\tau_\phi$  of the lower well when occupying the upper one out of resonance (see symbols in Fig. 8). It should be noted that Eq. (8) takes into account the interaction appearing in the singlet channel only. So, the possible reason for disagreement between the experimental data and calculation results is the neglecting of the contribution of the multiplet (with respect to spin and well isospin) channel in the dephasing rate. To our knowledge the role of the  $e$ - $e$  interaction in the multiplet channel in the dephasing in the double quantum well structures has not been studied yet in the literature.

Before concluding the paper, let us note that our results are in contradiction with those obtained in Ref. 13. In the structures with the relatively high interwell transition rate,

the authors observe the anomalous  $\sigma$  dependence of the dephasing time,  $\tau_\phi \sim \sigma^{-1}$ . This observation is inconsistent not only with the data in Fig. 8 but with the Fermi-liquid model,<sup>18</sup> which predicts  $\tau_\phi \sim \sigma$ . The possible reason is that the authors used the expression obtained in Ref. 11 for the case of identical wells, whereas the noticeable classical positive magnetoresistance observed at all the gate voltages fairly indicates that the mobilities in the wells are different.

#### IV. CONCLUSION

We have studied the interference quantum correction in the gated double quantum well  $\text{Al}_x\text{Ga}_{1-x}\text{As}/\text{GaAs}/\text{Al}_x\text{Ga}_{1-x}\text{As}$  heterostructures. Analyzing the positive magnetoconductivity we have obtained the interwell transition rate and the phase relaxation rate under the conditions when one and two quantum wells are occupied. It has been found that the interwell transition rate resonantly depends on the difference between the electron densities in the wells in accordance with the theoretical estimate. The central point of the paper, however, is that the dephasing rate in the lower quantum well is independent of whether the upper quantum well contributes to the conductivity or not. This observation is inconsistent with the results of simplest theory, which takes into account the inelasticity of the  $e$ - $e$  interaction in the singlet channel only, and predicts the increase in the dephasing time in double-layer structures as compared with the single-layer case. The further experimental and theoretical investigations are needed to find the answer to the question of whether the interaction in the multiplet channel or some other mechanism is responsible for such the feature of the dephasing processes in double quantum well structures.

#### ACKNOWLEDGMENTS

We would like to thank I. S. Burmistrov and I. V. Gornyi for illuminating discussions. This work has been supported in part by the RFBR (Grants No. 08-02-00662, No. 09-02-00789, No. 10-02-00481, and No. 10-02-91336).

<sup>1</sup>B. L. Altshuler and A. G. Aronov, in *Electron-Electron Interaction in Disordered Systems*, edited by A. L. Efros and M. Pollak (North-Holland, Amsterdam, 1985), p. 1.

<sup>2</sup>A. M. Finkel'stein, in *Electron-Electron Interaction in Disordered Systems*, edited by I. M. Khalatnikov (Harwood, London, 1990), Vol. 14.

<sup>3</sup>I. L. Aleiner, B. L. Altshuler, and M. E. Gershenson, *Waves Random Media* **9**, 201 (1999).

<sup>4</sup>G. Zala, B. N. Narozhny, and I. L. Aleiner, *Phys. Rev. B* **64**, 214204 (2001).

<sup>5</sup>I. V. Gornyi and A. D. Mirlin, *Phys. Rev. B* **69**, 045313 (2004).

<sup>6</sup>A. Punnoose and A. M. Finkel'stein, *Science* **310**, 289 (2005).

<sup>7</sup>G. M. Minkov, A. V. Germanenko, O. E. Rut, A. A. Sherstobitov, and B. N. Zvonkov, *Phys. Rev. B* **79**, 235335 (2009).

<sup>8</sup>G. M. Minkov, A. A. Sherstobitov, O. E. Rut, and A. V. Ger-

manenko, *Physica E* **25**, 42 (2004).

<sup>9</sup>G. M. Minkov, A. V. Germanenko, O. E. Rut, A. A. Sherstobitov, and B. N. Zvonkov, *Phys. Rev. B* **75**, 235316 (2007).

<sup>10</sup>N. S. Averkiev, L. E. Golub, and G. E. Pikus, *Fiz. Tekh. Poluprovodn.* **32**, 1219 (1998) [*Semiconductors* **32**, 1087 (1998)].

<sup>11</sup>O. E. Raichev and P. Vasilopoulos, *J. Phys.: Condens. Matter* **12**, 589 (2000).

<sup>12</sup>G. M. Minkov, A. V. Germanenko, O. E. Rut, O. I. Khrykin, V. I. Shashkin, and V. M. Daniltsev, *Nanotechnology* **11**, 406 (2000).

<sup>13</sup>I. R. Pagnossin, A. K. Meikap, T. E. Lamas, G. M. Gusev, and J. C. Portal, *Phys. Rev. B* **78**, 115311 (2008).

<sup>14</sup>E. Abrahams, S. V. Kravchenko, and M. P. Sarachik, *Rev. Mod. Phys.* **73**, 251 (2001).

<sup>15</sup>G. M. Minkov, A. V. Germanenko, V. A. Larionova, S. A. Ne-

- gashev, and I. V. Gornyi, *Phys. Rev. B* **61**, 13164 (2000).
- <sup>16</sup>A. V. Germanenko, V. A. Larionova, I. V. Gornyi, and G. M. Minkov, *Int. J. Nanosci.* **6**, 261 (2007).
- <sup>17</sup>G. M. Minkov, A. V. Germanenko, and I. V. Gornyi, *Phys. Rev. B* **70**, 245423 (2004).
- <sup>18</sup>B. N. Narozhny, G. Zala, and I. L. Aleiner, *Phys. Rev. B* **65**, 180202 (2002).
- <sup>19</sup>The numerical simulation shows that this conclusion is valid over the whole magnetic field range including the intermediate fields.
- <sup>20</sup>G. M. Minkov, A. V. Germanenko, O. E. Rut, O. I. Khrykin, V. I. Shashkin, and V. M. Daniltsev, *Phys. Rev. B* **62**, 17089 (2000).
- <sup>21</sup>Equation (8) has been derived by I. V. Gornyi and independently by I. S. Burmistrov and Y. Rodionov in framework of the random-phase approximation. They used the standard expression for  $\tau_\phi$  (Refs. 1 and 18), in which the effective dynamically screened interaction potential took into account both effects mentioned in the text: the inelastic interaction between the electrons in the different wells and the screening of the interaction between the electrons in the one well by the electrons located in the second one.